Life Sciences 217 (2019) 41–48

Contents lists available at ScienceDirect

Life Sciences

journal homepage: www.elsevier.com/locate/lifescie

pH and thermo dual stimulus-responsive liposome nanoparticles for targeted delivery of platinum-acridine hybrid agent

Qian Zhou, Chaoqun You, Yang Ling, Hongshuai Wu, Baiwang Sun*

School of Chemistry and Chemical Engineering, Southeast University, Nanjing 210096, PR China

ARTICLE INFO

Keywords:
Platinum-acridine complexes
Non-cisplatin-type
DNA binding
Anticancer agents
Nanocarrier

ABSTRACT

The complexes of the type $[PtCl(L2)(ACRAMTU)](NO_3)_2$ (ACRAMTU = 1-[2-(acridin-9-ylamino)ethyl]-1,3-dimethylthiourea) were synthesized: PT-ACRAMTU (**1**), L2 = ethane-1,2-diamine (en); PT(dach)-ACRAMTU (**2**), L2 = (1*R*,2*R*)-1,2-diaminocyclohexane (dach); PT(pda-OH)-ACRAMTU (**3**), L2 = 2-hydroxy-1,3-propanediamine (pda-OH). The complexes containing diverse diamines exhibit different DNA binding capacity and cytotoxicity. Complex **3** shows excellent capability not only on the strongest non-cisplatin-type DNA damage, but also superior anticancer activity in NCI-H460 cells (IC_{50} = 0.23 ± 0.05 μM). For overcoming water insolubly and side effects, we encapsulated complex **3** into liposomes. PT@NPs were characterized in terms of particle size, morphology, drug loading capacity (DLC), encapsulation efficiency (EE) and stability. *In vitro* triggered release showed that the release of the platinum drug was steerable and the release rate was fast under low pH (< 7.0) and high temperature (> T_m = 41 °C). PT@NPs showed significant inhibitory effect in NCI-H460 cells. Flow cytometry analysis indicates G0/G1 phase arrest of cells treated with complex **3**, whereas cells treated with cisplatin progress to G2/M of the cell cycle. The mechanistic differences validate that complex **3** is a potent anticancer agent superior than current clinical platinum-based therapies. PT@NPs have the potential in drug delivery systems (DDS) for non-small cell lung cancer (NSCLC) therapy.

1. Introduction

Cisplatin is a drug widely used in a variety of cancer treatment, but its application is limited for the side effects such as resistance, dose-dependent nephrotoxicity, neurotoxicity and emetogensis [1]. To solve these disadvantages of cisplatin, numerous analogues have been developed and evaluated to search for novel active agents [2].

DNA is the ultimate target of platinum drugs and DNA binding mode is a critical factor of platinum cytotoxicity [3]. Platinum compounds exert anticancer activity through the formation Pt-DNA adducts, resulting in DNA structural changes and activation of the cell death pathways such as apoptosis [4,5]. However, cellular resistance to platinum-based agents is a common feature in mammalian cells [6,7]. Resistance mechanisms are multifaceted and may involve low cellular uptake of drugs, and/or enhancement of DNA repair systems, or inactivation by high levels of cellular thiol containing molecules, such as glutathione or metallothioneine [7,8]. Therefore, one aim at developing new cancer therapeutics is making DNA structure change that is not recognized or repaired by DNA repair machinery, thus inducing cell apoptosis.

We have synthesized a series of acricine derivatives, and some of which exhibited excellent anticancer activity [9,10]. Platinum-acridine agents are derived from the prototypical complex PT-ACRAMTU, which target DNA through a dual binding mode involving intercalation and monofunctional platination of nucleobase nitrogen [11,12]. The formation rates of the hybrid adducts are significantly higher and DNA damages are more serious than the classical cross-links [13]. In addition, the hybrid adducts are significantly more potent inhibitors of RNA polymerase II than the cross-links [14]. The cumulative effects lead to cell cycle arrest in G1/S phase and efficiently trigger apoptosis of NSCLC models [15]. In the most sensitive cell lines, PT-ACRAMTU proved to be more active than cisplatin, and enhanced cytotoxicity was typically observed for the platinum-acridines compared to the platinum-free acridines [13]. The Pt—S linkage is resistant to nucleophilic attack by nucleobase nitrogen, causing ACRAMTU a typical non-leaving group. PT-ACRAMTU shows activity in a number of cancers including cisplatin sensitivity and resistant cancers, such as ovarian, colon, leukemic, nonsmall cell lung, and pancreatic cell lines [16–18].

Nanocarriers have attracted worldwide attention for use as carriers of chemotherapeutical drugs [19–24]. Nanocarriers have many superiorities, including enhanced endocytosis, prolonged circulation time, controlled drug release and so on [25–30]. Many studies showed that

* Corresponding author.
E-mail address: chmsunbw@seu.edu.cn (B. Sun).

https://doi.org/10.1016/j.lfs.2018.11.052
Received 22 August 2018; Received in revised form 22 November 2018; Accepted 23 November 2018
Available online 24 November 2018
0024-3205/

nanocarriers can significantly enhance the anticancer effect of the drugs in tumor tissues, for the accurate transportation [31–39]. Liposomes can effectively and controllably release drugs, for their good biocompatibility and brief surface functionalization [40,41].

To delineate structure-activity relationships within a series of platinum-acridine complexes, we synthesized a novel platinum-acridine agent **3**,and we used **1** and **2** to describe structure-activity relationships. The results demonstrate that the nature of diamines is a critical factor for the DNA binding and biological activity of these complexes, and complex **3** is an active anticancer agent. Then we selected an active complex **3** to build polymeric nanoparticles, using liposomes as the nanocarrier, and cyclic (Arg-Gly-Asp-$_D$-Phe-Lys) (cRGD) peptide as a targeted ligand, which exhibited a high affinity for $\alpha_v\beta_3$ integrins, an overexpressed protein in tumor cells. The results demonstrated that the targeted PT@NPs had a well-controllable drug release, and the potential for drug delivery system (DDS) for non-small cell lung cancer (NSCLC) therapy.

2. Material and methods

2.1. Synthesis of platinum-acridine compounds

All reagents were obtained from common vendors and used as obtained. The platinum precursors [Pt(L2)Cl_2] were prepared following the method described by Dhara [42,43]. [PtCl(L2)(ACRAMTU)]$(NO_3)_2$ were generated according to the procedures published earlier [16,44]. (Scheme 1).

2.2. Preparation of PT(pda-OH)-ACRAMTU loaded liposomes (PT@NPs)

The cRGD-PEG-PCL was synthesized according to our previous work [45]. Liposomes encapsulating were formulated using a film hydration method, according to the literature [46,47]. Briefly, SP (45 mg), cRGD-PEG-PCL (3 mg), and PT(pda-OH)-ACRAMTU (20 mg) were dissolved in acetonitrile, and a thin film was formed through reduced pressure distillation. The acetonitrile was completely removed in a vacuum drying oven. The film was added deionized water and ultrasonicated for 5 min. The suspension was shaken for 30 min at 30 °C to ensure well dispersed. The formation was centrifuged at 3000 rpm for 15 min, then filtered using a 0.22 μm filter (Millipore) and lyophilized.

2.3. Characterization of PT@NPs

The particle size distribution was measured using dynamic light scattering (DLS) at 25 °C, the samples were gradually squeezed out through 0.22 μm membrances after ultrasonic vibration for 5 min. Samples were diluted 2 fold with ultrapure water, then measured in triplicate. The particle size distribution data was generated using DTS Nano software. The liposome size polydispersity was indicated by the polydispersity index (PDI). The shape and surface morphology of the particle was visualized with a JEM-100CXII transmission electron microscope.

2.4. Drug loading capacity (DLC) and encapsulation efficiency (EE) of PT@NPs

The complex **3** was extracted from the dried drug-loaded liposomes with methanol, and the mass of PT@NPs was calculated using a high performance liquid chromatograph (HPLC) at 212 nm (comparing with complex **3** calibration curve, see Fig. S5). The drug loading capacity and encapsulation efficiency were calculated according to the following equations:

$$EE(\%) = \frac{\text{Weight of drug in NPs}}{\text{Weight of total drug}} \times 100\% \quad (1)$$

$$DLC(\%) = \frac{\text{Weight of drug in NPs}}{\text{Weight of PT@NPs}} \times 100\% \quad (2)$$

2.5. Stability of the liposomes

The stability of the prepared PT@NPs was evaluated within four weeks. The changes of particle size and PDI were analyzed using DLS. Liposomal samples were centrifuged at 1500 rpm for 10 min to ensure that impurities were sedimented. 3 mL aliquot taken from the supernate was measured using HPLC. Each sample was measured three times.

2.6. In vitro triggered release of liposomes

The PT(pda-OH)-ACRAMTU released from PT@NPs was measured through testing the platinum drug released from the liposomes [48]. We detected the pH (7.4, 7.2, 7.0, 6.8, 6.5 and 6.0) and the temperature (25, 37, 40, 42 and 45 °C) triggered release of liposomes. The solution was centrifuged at 1500 rpm for 15 min to make sure that the free PT(pda-OH)-ACRAMTU was sedimented. The supernate was collected,

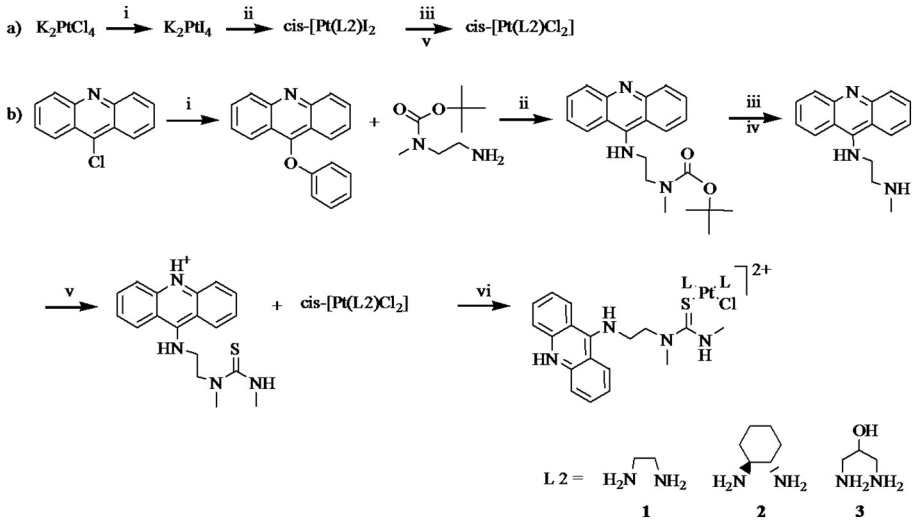

Scheme 1. Reagents and conditions: a) (i) KI, dark, rt.; (ii) L2; (iii) $AgNO_3$; (v) NaCl; b) (i) $NaOC_6H_5$, reflux; (ii) THF, reflux; (iii) HCl, CH_3COOH, rt.; (iv) 2 M NH_3, rt.; (v) MeNCS, EtOH, reflux; (vi) $AgNO_3$, DMF, dark, rt.

and filtered using a 0.22 μm filter in the dark, PT(pda-OH)-ACRAMTU mass loaded in the liposomes was calculated using HPLC at 212 nm.

To investigate the pH triggered releasing efficiency, three aliquots of PT@NPs were immersed in 2 mL of buffer solution at 25 °C of different pH values (7.4, 7.2, 7.0, 6.8, 6.5 and 6.0), which were shaken at a certain time interval. After centrifugation, the supernatant was added an equal volume of fresh medium to measure the absorption. Through comparing the absorption curve of pure PT(pda-OH)-ACRAMTU in different pH solutions, the amount of released PT(pda-OH)-ACRAMTU can be calculated.

The procedure for investigation the thermally stimulated release efficiency was quite same as that for pH triggered release investigation. We set different temperatures (25, 37, 40, 42 and 45 °C).

2.7. Gel electrophoresis

Gel electropboresis used Tris-HCl buffer (50 mM Tris/50 mM NaCl, pH 7.4) to treat the samples. The plasmid pUC18 DNA was treated by cisplatin and three complexes **1–3** with different concentrations. After the samples were incubated at 37 °C for 2 h, a loading buffer containing 25% bromophenol blue was added and electrophoresis was performed at 80 V for 0.5 h in TBE buffer using 1% agarose gel containing 1.0 μg/mL GelRed. Bands were visualized by UV light and photographed on a capturing system.

2.8. Circular dichroism (CD)

Circular dichroism (CD) was performed in Tris-HCl buffer (5 mM Tris/50 mM NaCl, pH 7.4). Solutions of calf thymus DNA (ctDNA) gave a ratio of UV absorbance at 260 and 280 nm of 1.8, indicating that the DNA was sufficiently free of protein. The concentration of ctDNA was determined spectrophotometrically using the molar absorption coefficient 6600 M^{-1} cm^{-1} at 260 nm. The stock solution was stored at 4 °C and used in 4 days. The CD spectras of ctDNA were recorded as follows. Each samples of ctDNA with different concentrations of the complexes **1–3** were incubated at 37 °C for 12 h in the dark and were scanned in the wavelength range of 220–320 nm, the buffer background was subtracted.

2.9. Cell culture

Breast cancer cell line MCF-7, human hepatocarcinoma cell line HepG2 and human non-small-cell lung carcinoma cell line NCI-H460 were purchased from the Type Culture Collection of the Chinese Academy of Sciences, Shanghai, China. With 10% (v/v) fetal bovine serum and antibiotics at 37 °C in an atmosphere of 5% CO_2, MCF-7 and HepG2 cells were cultured in DMEM, while NCI-H460 cells were cultured in RPMI-1640.

2.10. Cell viability assay

The viability of cells was measured with MTT assay according to the standard protocol with minor modifications [49]. Cell suspension was dispensed into 96-well plate (5×10^3 cells/well) and we pre-incubated the plate for 24 h, followed by treatment with various concentrations of the complexes **1–3** and PT@NPs for 48 h, with cisplatin as control. Next, 50 μL MTT in PBS was added to each well of the plate and then incubated at 37 °C for 2–3 h. The absorbance of each well at 590 nm was measured under a multimode plate reader (PerkinElmer, EnVision, USA). The results representing the average of 3 parallel samples were expressed as the relative percentage of cell growth inhibition.

2.11. Apoptosis induction

Phosphatidylserine externalization was measured using Annexin V-FITC/PI apoptosis detection kit (BD Pharmingen, San Jose, CA, USA) following the manufacturer's instructions. Briefly, NCI-H460 cells were seeded in 6-well plates, treated with complex **3**, PT@NPs and cisplatin at a concentration of 5 μM and incubated for 24 h. Cells treated with blank liposomes were used as control. Cells were washed with cold PBS and resuspended in 100 μL binding buffer and incubated with 5 μL Annexin-FITC and 10 μL PI in the dark for 15 min. Samples were tested using flow cytometry.

2.12. Cell cycle assay

NCI-H460 cells were treated for 24 h with complex **3**. Briefly, cells were collected and washed twice in PBS and then resuspended in 0.5 mL of staining buffer of propidium iodide (PI) in the dark for 30 min at room temperature. Nuclear PI fluorescence signal was recorded on the FL2-A channel of a FACS scan flow cytometer. The number of cells in G1, S and G2 phases was expressed as percentages of total events.

3. Results

3.1. Design and chemistry

Complexes **1–3** were synthesized according to the procedures published earlier [16,44]. The dach was introduced to alter flexibility and steric bulk in the ligand periphery. The pda-OH was chosen for its potential to be a donor or an acceptor for hydrogen bond, which could play an important part in binding the active part of platinum complexes with DNA of cancer cells. The complexes **1–3** were generated from the corresponding diaminedichloroplatinum(II) precursors after abstraction of one chloro using $AgNO_3$ followed by reaction with 1 equiv. of ACRAMTUHNO_3. All complexes were isolated as the water-soluble nitrate salts and characterized by ^{1}H NMR spectroscopy and Time of Flight Mass Spectrometry (Fig. S1 and S2).

3.2. Preparation and characterization of liposomes

Liposomes were prepared used the thin-film hydration method described in the previous literature. The schematic diagram of the procedure is presented in Fig. 1. In order to prepare liposomes with suitable particle size and good morphology, a series of experiments with different reactant ratios were carried out. Finally, we obtained liposomes with good sizes, which suitable for *in vivo* delivery. The prepared liposomes have a uniform spherical shape, with a mean size of around 97 nm, as shown in Fig. 2. The addition of phospholipids enhanced the stability of the prepared liposomes. The TEM image showed that the surface of the prepared liposomes was smooth.

The reactant formulas and the test results are listed in Table S1. The results exhibited the property of the liposomes, such as mean particle size, EE, DLC and PDI. The liposomes displayed well morphology homogeneity, with PDIs were below 0.3. The mean diameters increased from 75.12 to 116.57 nm with the increasing ratio of phospholipids.

3.3. DNA binding study

The DNA unwinding was measured on pUC18 supercoiled plasmid DNA by agarose gel electrophoresis. Intrastrand cross-links formed by cisplatin cause unwinding of DNA duplex by 13° at each platination site [50]. Incubation of pUC18 with various amounts of platinum-acridine hybrid agents are shown in Fig. S3. Three complexes show the differences in the relative degrees of the DNA unwinding compared to cisplatin. Complex **3** produces the most intense DNA damage, whereas the relaxed form produced by **2** results in less intense band on the gel compared to **1**.

The CD spectra of the series of complexes with 4×10^{-5} M B-form ctDNA showed positive bands at 275 nm due to base stacking and negative bands at 245 nm due to DNA right-handed helicity. (Fig. S4) The intensity of negative bands increased and slight red shifts were

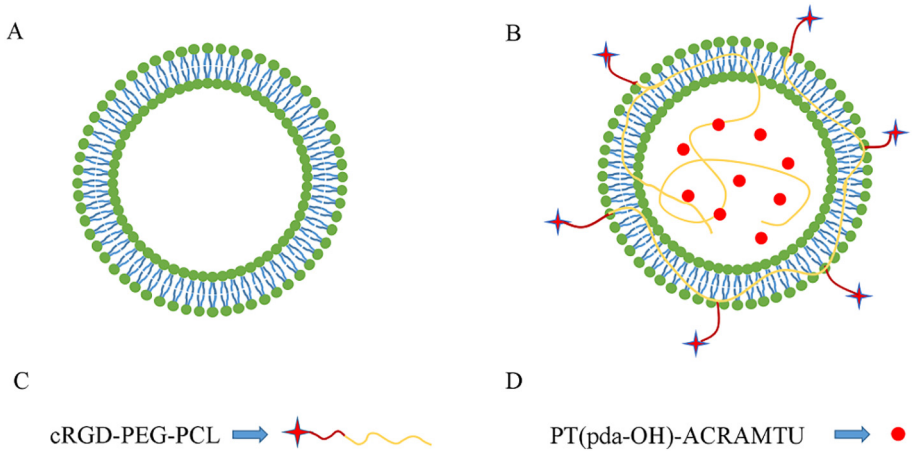

Fig. 1. (A) Pure phosphatide liposomes; (B) PT@NPs; (C) cRGD-PEG-PCL; (D) Complex **3**.

observed with increasing concentration of complexes. The intensity of positive bands at 275 nm also increased with no significant red shift when the concentration of complexes increased. The above enhancement of molar ellipticity at 275 nm indicated that the complexes interact with ctDNA, by intercalation or external binding. Slight red shifts suggest retention of the B-form conformation. The differences in enhancement of the bands at 275 nm are pronounced, indicating a difference in the extent of intercalation by the complexes. The order of increasing intercalation is **2** < **1** < **3**. Thus, the CD analysis revealed that the changing type of diamine nonleaving groups in PT-ACRAMTU analogues affect their binding interaction with DNA.

3.4. The stability of the liposomes

The stability of the liposomes was estimated on 0, 3, 7, 14, 21 and 28 days. At each time point, the PT@NPs was centrifuged at 1500 rpm for 10 min to make sure that the leaked PT(pda-OH)-ACRAMTU was precipitated. The supernatant was extracted and mixed with methanol separately, and centrifuged, and the PT(pda-OH)-ACRAMTU was calculated for each time point in triplicate using HPLC at 212 nm, comparing with the PT(pda-OH)-ACRAMTU calibration curve (Fig. S5). The results indicated that a large part of liposomes retained PT(pda-OH)-ACRAMTU without obvious leakage, and showed good stability as show in Fig. 3. The particle size and the EE showed slightly change. The results exhibited that the PT@NPs can show excellent stability for a certain period.

3.5. In vitro pH and temperature triggered release of liposomes

To investigate the pH-dependent release efficiency, the lipsome solution was divided into six aliquots and adjusted pH to 7.4, 7.2, 7.0, 6.8, 6.5 and 6.0. The solution was vibrated at certain time intervals. After centrifugation, the supernatant was added an equal volume of fresh medium, and taken out to measure the PT(pda-OH)-ACRAMTU content. By comparing with the absorption values from the PT(pda-OH)-ACRAMTU calibration curve, the amount of released PT(pda-OH)-ACRAMTU was calculated.

The results indicated that the liposomes exhibit pH-sensitive triggered release, as shown in Fig. 4A. The release process of PT(pda-OH)-ACRAMTU was monitored at certain time intervals over 24 h at 25 °C. The amounts of released PT(pda-OH)-ACRAMTU increased while the pH value reduced. At 24 h, 35.6% of PT(pda-OH)-ACRAMTU was released at pH = 7.4, while 84.5% of PT(pda-OH)-ACRAMTU was released at pH = 6.8, and the release amount of PT(pda-OH)-ACRAMTU obviously increased to 91.5% at pH = 5.0. This may be due to the addition of PEG-PCL to the lipid bilayer structure of phospholipids, which showed a tightly arranged state under neutral pH and changed to hydrophilic chain structure when the pH value was reduced.

To investigate the temperature triggered release of liposomes, we set different temperatures of 25, 37, 40, 42 and 45 °C in buffer solution at pH = 7.4. As shown in Fig. 4B, the release curves at different temperatures were obtained. The phase transition temperature (T_m) of our prepared liposomes is around 41 °C. After 24 h, the release efficiencies of PT(pda-OH)-ACRAMTU at 42 °C and 45 °C were 85.5% and 91.5%, much higher than which at 25 °C (39.6%). The liposomes sustained stable bilayer structure and the PT(pda-OH)-ACRAMTU leaked from the gaps of the lipid bilayer when the temperature was below T_m. However, when the temperature was reached and higher than T_m, the phospholipid structure began to depolymerize, which accelerated the release of PT(pda-OH)-ACRAMTU from the liposomes. The results showed that the release of PT@NPs is pH- and thermo-controllable.

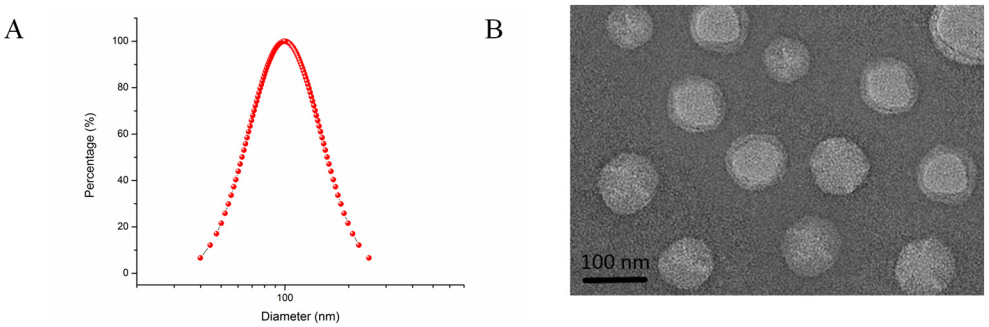

Fig. 2. (A) Statistical analysis of the sizes of PT@NPs measured from TEM images. (B) TEM image of PT@NPs.

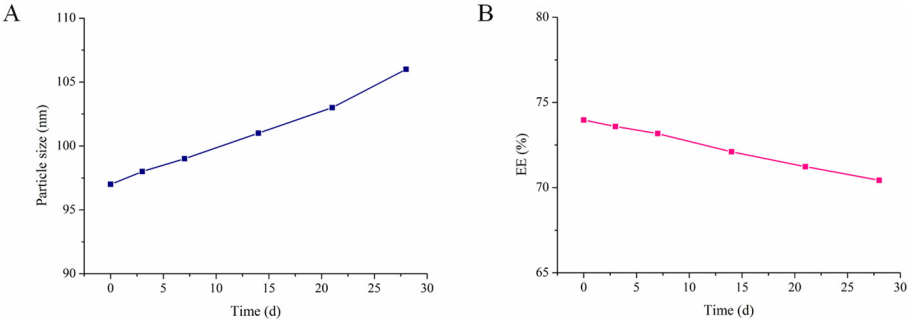

Fig. 3. The stability of the PT@NPs in 4 weeks: (A) the change of the mean particle size; (B) the change of the encapsulation efficiency.

3.6. Cell viability

The cytotoxic effect of the complexes **1–3** and PT@NPs were tested against HepG2, MCF-7 and NCI-H460 cells, cisplatin was used as positive control. The corresponding IC_{50} values are showed in Table 1, complexes **1** and **3** show a moderate enhancement of activity compared to cisplatin in HepG2 cells. However, complex **2** shows low cytotoxicity with IC_{50} (14.08 ± 1.43 μM) even higher than cisplatin (12.1 ± 0.9 μM) in MCF-7 cells. All complexes show pronounced enhanced cytotoxicity in NCI-H460 cells, an even more dramatic effect is observed for complex **3**. The new derivative **3** proves to be the potent antitumor drug.

To further investigate whether the cancer cells can be efficiently inhibited by the complexes, we incubated the complexes with HepG2, MCF-7 and NCI-H460 cells for 24 h at 37 °C, and the cytotoxicity of the complexes towards cancer cells was investigated with standard MTT assays (Fig. 5). For HepG2 and MCF-7 cells, the cytotoxicity of the complexes slightly increased compared with cisplatin. However, significant cytotoxicity was observed in NCI-H460 cells when the concentration of the complexes increased.

The liposome encapsulated complex **3** reduced the cytotoxicity of the complex **3**, the inhibitory effect of the PT@NPs was obviously lower than the free PT(pda-OH)-ACRAMTU. However, the PT@NPs showed excellent cytotoxicity in NCI-H460 cells, this may be for the reason that the NCI-H460 cells can absorb more amount of PT@NPs.

3.7. Apoptosis induction

To further investigate the induced apoptosis effects of the complex **3** and PT@NPs, Annexin V-FITC/PI assay was performed in NCI-H460 cells. As shown in Fig. 6, blank-liposome did not induce obvious cell apoptosis, with apoptosis rate of 9.1%. Compared with blank-liposome, NCI-H460 cells treated with cisplatin, complex **3** and PT@NPs resulted in 41.5%, 69.7% and 55.8% cells apoptosis. The PT@NPs mediated apoptosis was remarkable, only slightly lower than complex **3**.

Table 1
Summary of cytotoxicity datas (IC_{50}) for Platinum-Acridines and Cisplatin in Human Solid Tumor Cell Lines. IC_{50} values are mean ± SD from at least three independent experiments.

Compound	Cytotoxicity in different cell lines (IC_{50} ± SD, μM)		
	HepG2	MCF-7	NCI-H460
Cisplatin	19.2 ± 1.6	12.1 ± 0.9*	25.3 ± 1.8
Complex **1**	4.32 ± 0.21	2.54 ± 0.34*	0.83 ± 0.11*
Complex **2**	9.75 ± 0.84	14.08 ± 1.43	2.42 ± 0.25*
Complex **3**	3.68 ± 0.36*	5.75 ± 0.65	0.23 ± 0.05*
PT@NPs	12.39 ± 1.03	14.63 ± 0.89	3.13 ± 0.34*

* $p < 0.05$ compared to control.

3.8. Cell cycle

NCI-H460 cell death was induced more efficiently by complex **3** than cisplatin [17]. Thus, the effect of complex **3** on cell cycle progress was analyzed by flow cytometry. NCI-H460 cells were incubated with 5 μM complex **3** for 24 h along with untreated cells. Cisplatin-DNA adducts typically inhibit DNA replication to an extent that slow cell cycle progression through the S phase but allow cells to accumulate in the G2/M phase [51], as shown in Fig. 7B. Flow cytometry analysis of the complex **3** shows an accumulation of cells in the G1 phase but not in the G2 phase (Fig. 7C). The result shows a G0/G1 phase arrest of NCI-H460 cells treated with **3**, whereas cells treated with cisplatin progress to G2/M of the cell cycle [15].

4. Discussion

In this paper, we designed PT-ACRAMTU analogues as DNA-targeted agents structurally and functionally differ from cisplatin. PT-ACRAMTU-type compounds are believed to delay DNA processing enzymes by lengthening and unwinding DNA [52]. We evaluated the effects of variations on the diamine nonleaving groups in PT-ACRAMTU

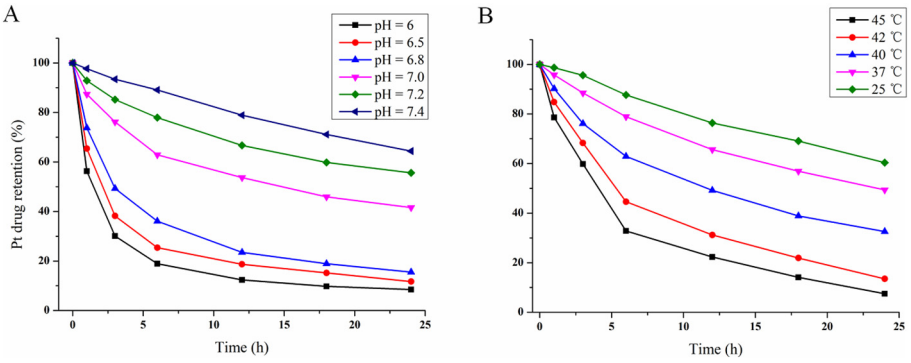

Fig. 4. (A) The pH-dependent release of PT@NPs at 25 °C; (B) The thermo-dependent release of PT@NPs at pH 7.4.

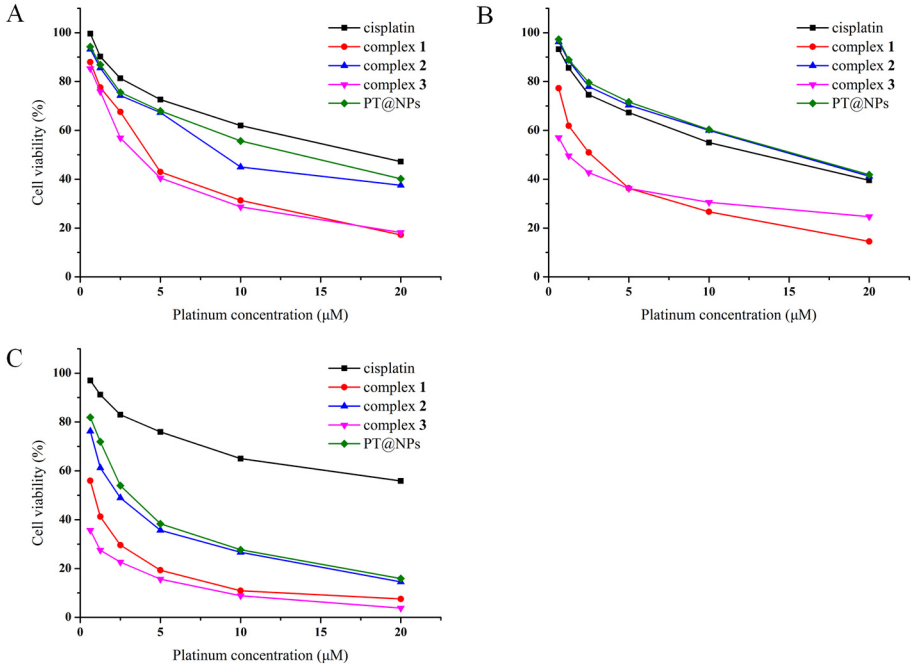

Fig. 5. Relative cell viabilities of HepG2 (A), MCF-7 (B) and NCI-H460 (C) cells after incubation with complexes for 24 h.

analogues, which affected DNA damage and anticancer activity. Bierbach et al. [16,17,44] have demonstrated that inactive derivatives can become lethal cytotoxins through simple chemical modification. The results showed that the diamine ligands in these PT-ACRAMTU analogues were indeed critical modulators of biological activity. Minor structural modifications of the diamine in PT-ACRAMTU derivatives may lead to a changed DNA damage profile and cytotoxicity. The hybrid agents produce more severe DNA damage than cisplatin. The complexes could induce HepG2, MCF-7 and NCI-H460 cells death, and showed the best growth inhibitory activity against NCI-H460 cells. In particular, replacing the en chelate of PT-ACRAMTU by a pda-OH group, resulted in the most active complex **3,** which exhibited higher anticancer activity by affecting cell proliferation and cell cycle distribution. The limited SAR suggested the importance of hydroxyl functionality for the cytotoxicity in the PT-ACRAMTU analogues.

Intercalations show moderate cytotoxicity, such as platinum-free acridines [9,10,17,44]. In our previous work, the acridine compounds show a good inhibitory activity on breast cancer cells, with IC_{50} values in the micromolar concentration [9,10]. PT-ACRAMTU and some of its derivatives show promising anticancer activity in a broad spectrum of cancer cells, with IC_{50} values in the low-micromolar and submicromolar concentration [11,13,16,53]. In the most sensitive cell line, most of the PT-ACRAMTU type complexes show stronger cytotoxicity than cisplatin and platinum-free acridines [16]. Complex **3** is remarkably cytotoxic in NCI-H460 cells. BBR3464, a trinuclear platinum complex in clinical trials, is a platinum-based complex which inhibits NCI-H460 cell

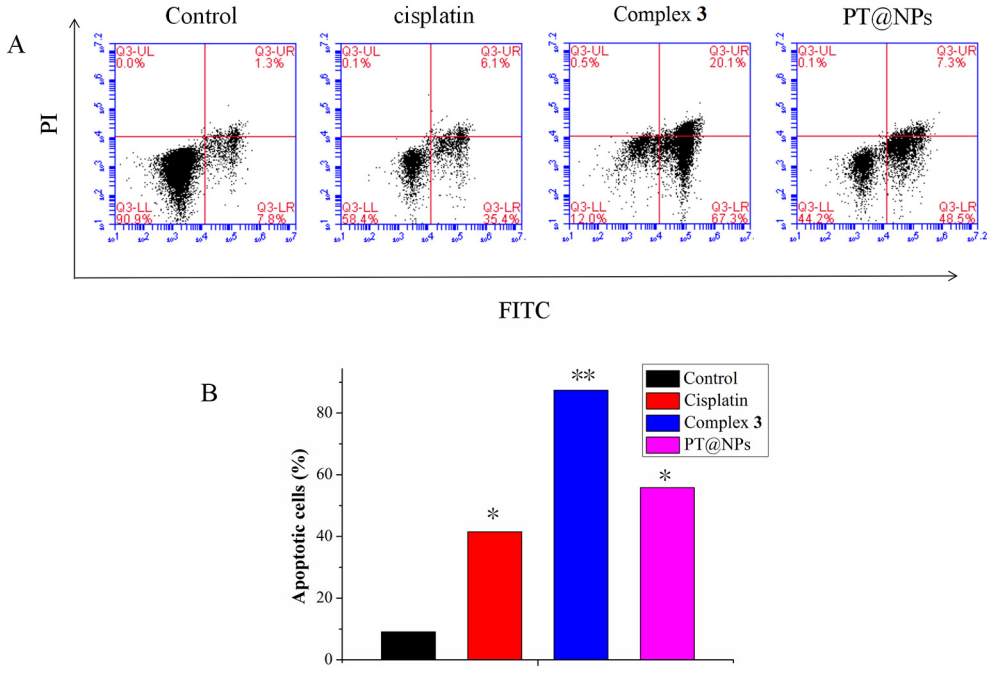

Fig. 6. Apoptosis induced by complexes in NCI-H460 cells. (A) Flow cytometric analysis of phosphatidylserine externalization (Annexin-V binding) and cell membrane intergrity (PI staining). (B) The percentage of apoptotic cells is calculated as the percentage of apoptotic cells in early and later stage. Data represent the mean value and SD from three independent experiments. *p < 0.05, **p < 0.01, *versus* control.

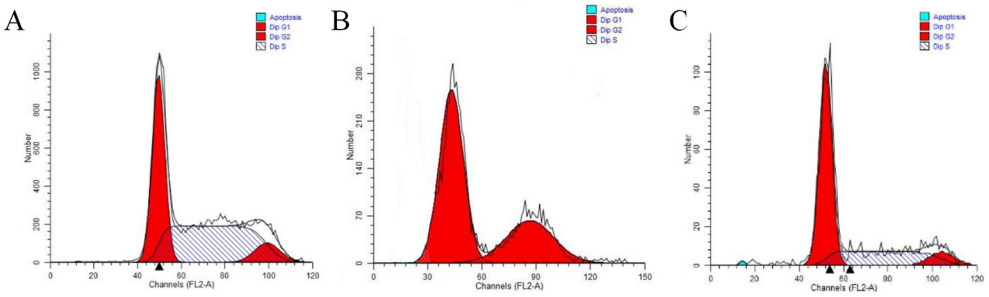

Fig. 7. (A) Cell cycle analysis of untreated NCI-H460 cells, (B) NCI-H460 cells treated with 5 μM cisplatin and (C) NCI-H460 cells treated with 5 μM complex **3** for 24 h. The percentages given are average values of three incubations.

proliferation with similar potency [54].

The active complex **3** was encapsulated into liposomes for delivery in cancer therapy. The PT@NPs showed the appropriate size of around 97 nm and spherical morphology. The EE and DLC of PT@NPs were 73.97% and 32.43%. The PT@NPs showed excellent stability, with slight change in the particle size and EE in four weeks. The pH and temperature triggered release of the liposomes showed that the release of the Pt drug was steerable, the release rate was fast under low pH and high temperature. Thus, the prepared liposomes can release slowly in normal tissues, and release rapidly in tumor tissue. In MTT assay, the PT@NPs also showed excellent cytotoxicity in NCI-H460 cells.

In conclusion, a noncross-linking agent based on platinum is able to generate a significant cell death compared to cisplatin in NCI-H460 cells, which is mediated by weakened DNA repair mechanism. Thus, PT-ACRAMTU derivatives may be effective chemotherapy anticancer agents in the treatment of some cancers, and they are potential to overcome tumor resistance to cisplatin. For overcoming the water insolubly and side effects, we encapsulated complex **3** into liposome. The features presented by PT@NPs in our work demonstrate that they have the potiential in drug delivery systems (DDS) for non-small cell lung cancer (NSCLC) therapy.

Acknowledgements

We gratefully acknowledge A Project Funded by the Priority Academic Program Development of Jiangsu Higher Education Institutions (PAPD).

Conflict of interest

The authors declare that there are no conflicts of interest related to this work.

Appendix A. Supplementary data

Supplementary data to this article can be found online at https://doi.org/10.1016/j.lfs.2018.11.052.

References

[1] E. Wong, C.M. Giandomenico, Current status of platinum-based antitumor drugs, Chem. Rev. 99 (1999) 2451–2466.
[2] Y.P. Ho, S.C.F. Au-Yeung, To KKW, Platinum-based anticancer agents: innovative design strategies and biological perspectives, Med. Res. Rev. 23 (2003) 633–655.
[3] D. Xu, Y. Min, Q. Cheng, et al., Chemical and cellular investigations of trans-ammine-pyridine-dichlorido-platinum(II), the likely metabolite of the antitumor active cis-diammine-pyridine-chorido-platinum(II), J. Inorg. Biochem. 129 (2013) 15–22.
[4] L. Kelland, The resurgence of platinum-based cancer chemotherapy, Nat. Rev. Cancer 7 (2007) 573–584.
[5] D. Wang, S.J. Lippard, Cellular processing of platinum anticancer drugs, Nat. Rev. Drug Discov. 4 (2005) 307–320.
[6] P. Heffeter, U. Jungwirth, M. Jakupec, et al., Resistance against novel anticancer metal compounds: differences and similarities, Drug Resist. Updat. 11 (2008) 1–16.
[7] D.J. Stewart, Mechanisms of resistance to cisplatin and carboplatin, Crit. Rev. Oncol. Hematol. 1 (2007) 12–31.
[8] G. Singh, A. Dorward, R. Moorehead, et al., Novel mechanisms of resistance to cancer chemotherapy, Cancer J. 8 (1995) 304–307.
[9] Q. Zhou, C.Q. You, C. Zheng, et al., 3-nitroacridine derivatives arrest cell cycle at G0/G1 phase and induce apoptosis in human breast cancer cells may act as DNA-target anticancer agents, Life Sci. 206 (2018) 1–9.
[10] Q. Zhou, H.S. Wu, C.Q. You, et al., 1,3-dimethyl-6-nitroacridine derivatives induce apoptosis in human breast cancer cells by targeting DNA, Drug Dev. Ind. Pharm. (2018), https://doi.org/10.1080/03639045.2018.1529185.
[11] R. Guddneppanavar, U. Bierbach, Adenine-N3 in the DNA minor groove-an emerging target for platinum containing anticancer pharmacophores, Anti Cancer Agents Med. Chem. 7 (2007) 125–138.
[12] L.A. Graham, J. Suryadi, T.K. West, et al., Synthesis, aqueous reactivity, and biological evaluation of carboxylic acid ester-functionalized platinum-acridine hybrid anticancer agents, J. Med. Chem. 55 (2012) 7817–7827.
[13] J. Suryadi, U. Bierbach, DNA metalating-intercalating hybrid agents for the treatment of chemoresistant cancers, Chem. Eur. J. 18 (2012) 12926–12934.
[14] H. Kostrhunova, J. Malina, A.J. Pickard, et al., Replacement of a thiourea with an amidine group in a monofunctional platinum-acridine antitumor agent. Effect on DNA interactions, DNA adduct recognition and repair, Mol. Pharm. 8 (2011) 1941–1954.
[15] C.L. Smyre, G. Saluta, T.E. Kute, et al., Inhibition of DNA synthesis by a platinum-acridine hybrid agent leads to potent cell kill in non-small cell lung cancer, ACS Med. Chem. Lett. 2 (2011) 870–874.
[16] E.T. Martins, H. Baruah, J. Kramarczyk, et al., Design, synthesis, and biological activity of a novel non-cisplatin-type platinum-acridine pharmacophore, J. Med. Chem. 44 (2001) 4492–4496.
[17] M.C. Ackley, C.G. Barry, A.M. Mounce, et al., Structure-activity relationships in platinum-acridinylthiourea conjugates: effect of the thiourea nonleaving group on drug stability, nucleobase affinity, and in vitro cytotoxicity, J. Biol. Inorg. Chem. 9 (2004) 453–461.
[18] S.M. Hess, A.M. Mounce, R.C. Sequeira, et al., Platinum-acridinylthiourea conjugates show cell line specific cytotoxic enhancement in H460 lung carcinoma cells compared to cisplatin, Cancer Chemother. Pharmacol. 56 (2005) 337–343.
[19] Q. Cheng, Y. Liu, Multifunctional platinum-based nanoparticles for biomedical applications, Wiley Interdiscip. Rev. Nanomed. Nanobiotechnol. 9 (2) (2017) 1–27.
[20] E. Ye, X.J. Loh, Polymeric hydrogels and nanoparticles: a merging and emerging field, Aust. J. Chem. 66 (9) (2013) 997–1007.
[21] X.J. Loh, T.C. Lee, Q. Dou, et al., Utilising inorganic nanocarriers for gene delivery, Biomater. Sci. 4 (1) (2015) 70–84.
[22] C. Dhand, N. Dwivedi, X.J. Loh, et al., ChemInform abstract: methods and strategies for the synthesis of diverse nanoparticles and their applications: a comprehensive overview, ChemInform 47 (9) (2015) 105003–105037.
[23] B.M. Teo, X.J. Loh, Magnetic anisotropic particles: toward remotely actuated applications, Part. Part. Syst. Charact. 33 (10) (2016) 709–728.
[24] C.Q. You, H.S. Wu, M.X. Wang, et al., Near-infrared light and pH dual-responsive targeted drug carrier based on core-crosslinked polyaniline nanoparticles for intracellular delivery of cisplatin, Chem. Eur. J. 23 (2017) 5352–5360.
[25] Y.F. Li, C. Chen, Fate and toxicity of metallic and metal-containing nanoparticles for biomedical applications, Small 7 (21) (2011) 2965–2980.
[26] J.H. Gao, H. Gu, B. Xu, Multifunctional magnetic nanoparticles: design, synthesis, and biomedical applications, Acc. Chem. Res. 42 (19) (2009) 1097–1107.
[27] M.R. Jones, K.D. Osberg, R.J. Macfarlane, et al., Templated techniques for the synthesis and assembly of plasmonic nanostructures, Chem. Rev. 111 (6) (2011) 3736–3827.
[28] S.A. Khan, A.K. Singh, D. Senapati, et al., Targeted highly sensitive detection of multi-drug resistant Salmonella DT104 using gold nanoparticles, Chem. Commun. 47 (33) (2011) 9444–9446.
[29] R. Lakshminarayanan, X.J. Loh, S. Gayathri, et al., Formation of transient amorphous calcium carbonate precursor in quail eggshell mineralization: an in vitro study, Biomacromolecules 7 (11) (2006) 3202–3209.
[30] R. Lakshminarayanan, E.Q. Chijin, X.J. Loh, et al., Purification and characterization of a vaterite-inducing peptide, pelovaterin, from the eggshells of Pelodiscus sinensis (Chinese soft-shelled turtle), Biomacromolecules 6 (3) (2005) 1429–1437.
[31] C.Q. You, M.X. Wang, H.S. Wu, et al., Near infrared radiated stimulus-responsive liposomes based on photothermal conversion as drug carriers for co-delivery of CJM126 and cisplatin, Mater. Sci. Eng. C 80 (2017) 362–370.
[32] C.Q. You, H.S. Wu, M.X. Wang, et al., A strategy for photothermal conversion of

polymeric nanoparticles by polyaniline for smart control of targeted drug delivery, Nanotechnology 28 (2017) 165102–165113.
[33] F. Zhao, Y. Zhao, X. Chang, et al., Cellular uptake, intracellular trafficking, and cytotoxicity of nanomaterials, Small 7 (10) (2011) 1322–1337.
[34] Y. Wang, Q. Zhu, L. Tao, et al., Controlled-synthesis of NiS hierarchical hollow microspheres with different building blocks and their application in lithium batteries, J. Mater. Chem. 21 (25) (2011) 9248–9254.
[35] K. Boubbou, A.C. Gruden, X.F. Huang, Magnetic glyco-nanoparticles: a unique tool for rapid pathogen detection, decontamination, and strain differentiation, J. Am. Chem. Soc. 129 (44) (2007) 13392–13393.
[36] Q.Q. Dou, X. Fang, S. Jiang, et al., Multi-functional fluorescent carbon dots with antibacterial and gene delivery properties, RSC Adv. 5 (58) (2015) 46817–46822.
[37] K. Huang, Q. Dou, J.L. Xian, Nanomaterial mediated optogenetics: opportunities and challenges, RSC Adv. 6 (2016) 60896–60906.
[38] H.C. Guo, E. Ye, Z. Li, et al., Recent progress of atomic layer deposition on polymeric materials, Mater. Sci. Eng. C 70 (2017) 1182–1191.
[39] Z. Li, E. Ye, R. Lakshminarayanan, et al., Recent advances of using hybrid nanocarriers in remotely controlled therapeutic delivery, Small 12 (35) (2016) 4782–4806.
[40] A.M. Chen, M. Zhang, D. Wei, et al., Co-delivery of doxorubicin and Bcl-2 siRNA by mesoporous silica nanoparticles enhances the efficacy of chemotherapy in multidrug-resistant cancer cells, Small 5 (23) (2009) 2673–2677.
[41] D. Peer, P.C. Zhu, C.V. Carman, et al., Selective gene silencing in activated leukocytes by targeting siRNAs to the integrin lymphocyte function-associated antigen-1, Proc. Natl. Acad. Sci. U. S. A. 104 (10) (2007) 4095–4100.
[42] S.C. Dhara, A rapid method for the synthesis of cis-[$Pt(NH_3)_2Cl_2$], Indian J. Chem. 8 (1970) 193–194.
[43] W.P. Liu, X.Z. Chen, M.J. Xie, et al., Synthesis and anticancer activity of [2-hydroxy-1,3-diaminopropane-κ2N,N′] platinum(II) complexes, J. Inorg. Biochem. 102 (2008) 1942–1946.
[44] R. Guddneppanavar, J.R. Choudhury, A.R. Kheradi, et al., Effect of the diamine nonleaving group in platinum-acridinylthiourea conjugates on DNA damage and cytotoxicity, J. Med. Chem. 50 (2007) 2259–2263.
[45] C.Q. You, H.S. Wu, M.X. Wang, et al., Co-delivery of cisplatin and CJM-126 via photothermal conversion nanoparticles for enhanced synergistic antitumor efficacy, Nanotechnology 29 (2018) 015601–015613.
[46] C.Q. You, J. Yu, Y. Sun, et al., Enhanced cytotoxicity by a benzothiazole-containing cisplatin derivative in breast cancer cells, New J. Chem. 41 (2017) 773–785.
[47] K. Virender, M. Goutam, S. Paige, et al., Codelivery of small molecule hedgehog inhibitor and miRNA for treating pancreatic cancer, Mol. Pharm. 12 (4) (2015) 1289–1298.
[48] X. Wu, Z.Y. Wang, D. Zhu, et al., pH and thermo dual-stimuli-responsive drug carrier based on mesoporous silica nanoparticles encapsulated in a copolymer-lipid bilayer, ACS Appl. Mater. Interfaces 5 (21) (2013) 10895–10903.
[49] X.Z. Chen, M.J. Xie, W.P. Liu, et al., Synthesis and structure of platinum(II) complexes containing an asymmetric chelating diamine 2-morpholinoethylamine as the carrier, Inorg. Chim. Acta 360 (2007) 2851–2856.
[50] M.V. Keck, S.J. Lippard, Unwinding of supercoiled DNA by platinum-ethidium and related complexes, J. Am. Chem. Soc. 114 (1992) 3386–3390.
[51] C.M. Sorenson, A. Eastman, Mechanism of cis-diamminedichloroplatinum(II)-induced cytotoxicity: role of G2 arrest and DNA double-strand breaks, Cancer Res. 48 (1988) 4484–4488.
[52] H. Baruah, C.L. Rector, S.M. Monnier, et al., Mechanism of action of non-cisplatin type DNA-targeted platinum anticancer agents: DNA interactions of novel acridinylthioureas and their platinum conjugates, Biochem. Pharmacol. 64 (2002) 751.
[53] Z. Ma, G. Saluta, G.L. Kucera, et al., Effect of linkage geometry on biological activity in thiourea- and guanidine-substituted acridines and platinum-acridines, Bioorg. Med. Chem. Lett. 18 (2008) 3799–3801.
[54] C. Manzotti, G. Pratesi, E. Menta, et al., BBR3464: a novel triplatinum complex, exhibiting a preclinical profile of antitumor efficacy different from cisplatin, Clin. Cancer Res. 6 (2000) 2626–2634.